

# Energy Conversion in a Solid-Particle-Entrained Gas That Expands Isothermally Through a Nozzle

C. A. Ordonez,\* E. D. Lessmann,† and D. L. Weathers‡

*University of North Texas, Denton, Texas 76203*

M. J. Traum,§

*Milwaukee School of Engineering, Milwaukee, Wisconsin 53202*

Initial research is reported regarding the expansion and energy conversion of a gas-solid two-phase flow. The multiphase fluid is expanded under conditions in which the energy of compressed gas is converted into kinetic energy of solid particles. Sufficient heat exchange between the gas and solid phases occurs for the gas phase expansion to proceed isothermally. A low-speed turbine is used to convert the kinetic energy of the solid phase into other forms. The speed of the solid phase after expansion is sufficiently small to avoid significant turbine erosion under the conditions studied.

## I. Introduction

A compressed-gas energy conversion system that employs a low-speed turbine is illustrated conceptually in Fig. 1. The energy conversion process that is implemented by the system can be divided into steps. In the first step of the process, compressed gas energy is converted into solid-particle kinetic energy, while the two-phase fluid accelerates downward through a nozzle. Heat exchange between the gas and solid phases causes the gas phase expansion to proceed isothermally. In the second step of the process, solid-phase kinetic energy is converted into mechanical motion using a turbine. With particles that are essentially incompressible and that travel at a speed much slower than the speed of sound, a low-speed turbine for use with incompressible fluids is suitable. At low power, a low-speed turbine may provide a significant cost advantage in comparison to a conventional high-speed turbine. In the third step of the process, the particles are separated from the expanded gas and recycled. For the particles to be recycled, they must be returned to the initial thermodynamic state in which they are mixed with compressed gas to form a multiphase fluid. One possible configuration (not shown) incorporates two hoppers that are cyclically pressurized out of phase. A hopper would be refilled at times when the hopper is depressurized. Energy must be expended to refill and re-pressurize each hopper, and the associated energy costs must be taken into account for experimentally evaluating the overall energy conversion efficiency of the integrated system. To achieve isothermal expansion, heat must be transferred from the solid phase to the gas phase. In effect, the particles are cooled slightly by the interaction. For continuous operation using an ambient-temperature compressed gas, the particles are reheated by heat exchange with an ambient-temperature thermal reservoir, while being transported back to the hopper. For example, heat exchange with atmospheric air may be used as part of a pneumatic conveyance setup that serves as the particle pump.

---

\*Professor, Department of Physics, AIAA Senior Member.

†Undergraduate Student, Department of Mechanical and Energy Engineering.

‡Associated Professor, Department of Physics.

§Assistant Professor, Department of Mechanical Engineering, 1025 N. Broadway, AIAA Member.

Experimentation with an apparatus that achieves the three-step process has been initiated, although the third step is carried out manually at present. Conversion of the energy of compressed gas has been clearly demonstrated experimentally using a turbine to convert the kinetic energy of particles into other forms. Experimental temperature measurements indicate that the expansion is describable as isothermal for the conditions studied. Turbine erosion rate measurements indicate tolerable erosion rates may be possible. It is anticipated that gas expansion and energy conversion in a multiphase fluid may eventually serve for converting compressed gas energy into other forms with high efficiency. Guidance for the current research is provided by the existing knowledge base on gas-solid flows (see, for example, Ref. 1), and by studies on erosion caused by two-phase flow,<sup>2-14</sup> on multiphase flow in vertical channels,<sup>15</sup> on pneumatic conveyance,<sup>16</sup> and on abrasive air jets.<sup>5</sup> In the long term, the energy conversion process described here may be suited for incorporation into energy systems that involve gas phase energy conversion. Of particular note is a system dubbed a “cryogenic heat engine.” Such a heat engine converts ambient heat, such as heat from the atmosphere, into useful work by employing a cryogenic-temperature substance as a heat sink. Some of the associated research has been described in Refs. 17-26.

## II. Energy Conversion Efficiency

An experimental effort has been initiated to evaluate the energy conversion efficiency that can be achieved by a system similar to that illustrated in Fig. 1. The operating parameters are chosen such that temperature measurements indicate that the gas phase changes temperature by less than 10% of the change that would be expected from an ideally reversible adiabatic expansion. The apparatus used for experimentation is conceptually describable by Fig. 1, except that the particles are manually loaded into the hopper. After the hopper is manually loaded, it is pressurized with compressed air, and the pressure is maintained constant during the time that two-phase fluid is allowed to flow through the nozzle. An issue with the present operation is that the flow must be carefully monitored to avoid allowing free air flow to commence as a result of a depletion of the solid phase. Free flowing air might increase the speed of the turbine employed to the point of catastrophic failure.

The particles employed in the experiment are cast stainless steel. We took optical images that included 95 unique particles, and we used ImageJ<sup>27</sup> from NIH to determine the characteristic diameter of each particle assuming each one is a sphere. The particles had a mean diameter of 156  $\mu\text{m}$ , with a standard deviation of 49  $\mu\text{m}$ . The particles are large enough for gravity and filtration to be used to separate the particles from the expanded gas.

Figures 2 and 3 show high-speed photographs of the two-phase fluid passing through a 6-bladed axial rotor with a 6.5 cm diameter and 13 cm pitch. The turbine breaks the fluid stream into separated portions.

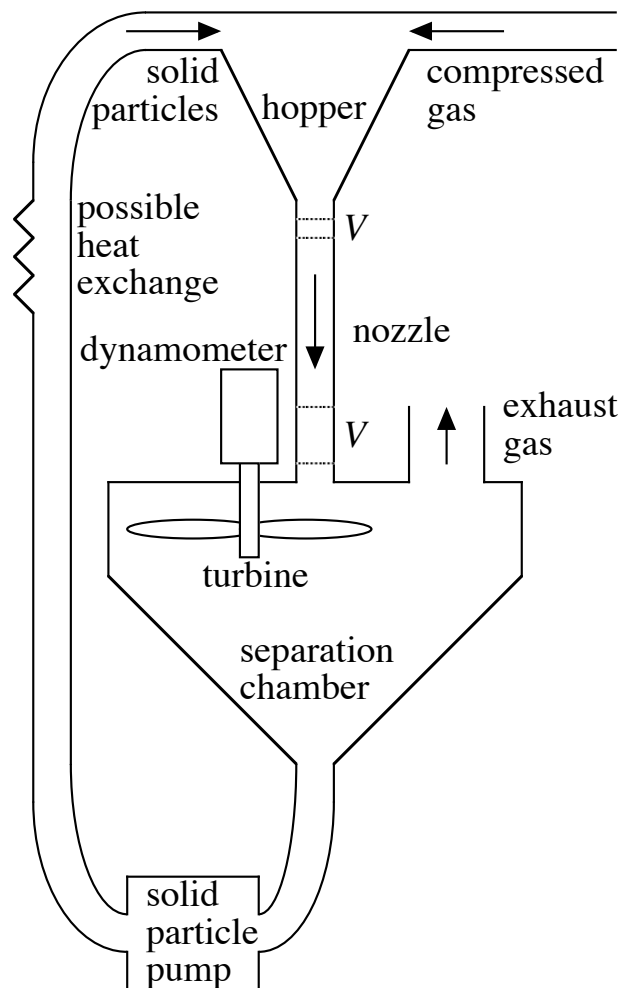


Figure 1. Conceptual illustration of a compressed gas energy conversion system that employs a low-speed turbine. The dynamometer can be replaced (e.g., by an electric generator, mechanical transmission, or hydraulic pump), depending on the form of output energy desired. A volume  $V$  of multiphase fluid increases as it accelerates down the nozzle.

Together with knowledge of the rotation speed of the turbine, the distance between breaks in the stream is used to determine the speed of the two-phase fluid after exiting the nozzle. A problem encountered is that at higher gas pressures, the spatial period of the stream variation is difficult to determine.

Figure 3 shows a photograph of the two-phase stream with a hopper pressure of 377 kPa. The distance between breaks in the stream was determined to be  $\sim 3$  cm, based in part on comparisons with other photographs taken under various operating conditions. As can be seen in the photograph, a tachometer was used to determine that the rotation speed of the turbine was 2585 rpm. A speed  $v = 7.8$  m/s is determined for the particles as they exit the nozzle. The nozzle is made of 304 stainless steel, is cylindrical in shape, and has a 15.24 cm length and a 0.96 cm inner diameter. The speed is calculated as  $v = N\Delta x f$ , where  $N = 6$  is the number of turbine blades,  $\Delta x = 0.03$  m is the spatial period of the stream variation, and  $f = 43.1$  Hz is the turbine rotation frequency. The time period during which flow was allowed to occur was  $\Delta t = 3.27$  s, and during that time, a measured mass  $M_s = 2.55$  kg of particles passed through the nozzle. The mass flow rate of the solid phase is  $\dot{m}_s = M_s/\Delta t = 0.78$  kg/s. The mass flow rate of the gas phase was measured to be  $\dot{m}_g = 8 \times 10^{-4}$  kg/s. The converted specific energy is defined as the kinetic energy of the solid component of the fluid exiting the nozzle per unit mass of the gas within it. The converted fluid specific energy is determined to be

$$w_e = \frac{(1/2)\dot{m}_s v^2}{\dot{m}_g} = 30 \text{ kJ/kg}$$

The theoretical maximum specific work available from the compressed gas for ideal expansions that are isothermal, adiabatic, and isobaric are calculated as  $w_i = (kT_i/m_g) \ln(p_i/p_f) = 110$  kJ/kg,  $w_a = (kT_i/m_g)(1/\epsilon)[1 - (p_i/p_f)^{-\epsilon}] = 93$  kJ/kg, and  $w_b = (kT_i/m_g)[1 - (p_i/p_f)^{-1}] = 62$  kJ/kg, respectively. Here,  $T_i = 296$  K is the temperature of the fluid prior to expansion,  $k$  is Boltzmann's constant,  $m_g$  is the average mass of a gas molecule (taken to be 28.96 amu for air),  $p_i = 377$  kPa is the gas pressure prior to expansion,  $p_f$  is the final pressure of the gas (taken to be atmospheric pressure),  $\epsilon = 1 - (1/\gamma)$ , and  $\gamma = 1.4$  for a diatomic gas. The isobaric expansion specific work is defined as the gauge pressure of the compressed gas multiplied by the volume per unit mass of the compressed gas. For deriving the specific work associated with the adiabatic and isothermal expansion processes, the work done on the atmosphere during the expansion and the work associated with gas injection into the hopper are taken into account. The two associated terms cancel out for the isothermal expansion expression, but not for the adiabatic expansion expression.

For an initial gas pressure  $p_i = 377$  kPa, an ideal adiabatic expansion would cause the temperature of the expanded gas to decrease by 90 K. Temperature measurements indicate that the expansion is describable as isothermal for the conditions studied. The efficiency of converting the compressed gas energy into kinetic energy relative to an ideal isothermal expansion process is determined to be  $e_i = w_e/w_i = 27\%$ .



Figure 2. High-speed photograph of two-phase fluid passing through a turbine.

In future work, we plan to employ higher gas pressures, where the effect of gravity can be neglected. The method described above that gives a fluid specific energy of 30 kJ/kg excludes the effect of gravity. We have gone over the conversion efficiency to try to include the power input due to gravity and to obtain a more accurate conversion efficiency. Here is our general approach: (1) Under unpressurized, gravity-flow conditions, determine the speed of the particles at a point just below the turbine. (2) Calculate an effective starting height above this point from which the particles would have to fall freely from rest to acquire this speed. (3) Apply this same effective starting height to the case of pressurized flow, and calculate the corresponding power input from gravity. (4) Subtract this power from the overall power in the particle stream to determine the power imparted by energy transfer from the compressed gas.

We used a photograph of the flow stream similar to Fig. 2 for unpressurized flow through a 0.96 cm-i.d. nozzle, 15.24 cm long. Duplicating the calculation above, we estimated the edges of the interrupted flow to be at  $y_1 = 54.9 \pm 0.1$  cm and  $y_2 = 50.0 \pm 0.1$  cm. The tachometer shows a frequency of  $f = 499$  rpm in the photograph, so the time interval for particles to travel from  $y_1$  to  $y_2$  is  $\Delta t = 10/f = 0.02004$  s. Using  $y_2 - y_1 = v_1 \Delta t + (1/2)g(\Delta t)^2$  to solve for  $v_1$ , we found a speed  $v_1 = 2.35 \pm 0.07$  m/s at position  $y_1$ , which is 7 cm below the lower end of the nozzle.

We then calculated the height from which the particles would have to fall starting from rest to reach this speed, using  $v_1^2 = 2gh$ , and found  $h = 28 \pm 2$  cm, or an effective starting height of  $21 \pm 2$  cm above the bottom of the nozzle. [Two comments here: (i) we included an estimate for an initial velocity  $v_0$  of the particles in the hopper of 0.2 m/s based on a 15.0 ml/s flow rate of the tightly-packed particles from the hopper through the 0.96 cm-diameter orifice, but this only made about a 2 mm difference in the height estimate, which is negligible given the overall uncertainty. (ii) This 21 cm height coincides with the center of a valve that is located just above the top of the nozzle, and so makes some physical sense as a point from which the particles would begin to move freely in their descent through the nozzle.]

We then used the image of the pressurized flow shown in Fig. 3 to reproduce the speed calculation for that measurement. We estimated the edges of the interrupted flow to be at  $y_1 = 58.2 \pm 0.1$  cm and  $y_2 = 55.3 \pm 0.1$  cm. The tachometer shows a frequency of  $f = 2585$  rpm in the photograph, so the time interval for particles to travel from  $y_1$  to  $y_2$  is  $\Delta t = 10/f = 0.003868$  s. Again using  $y_2 - y_1 = v_1 \Delta t + (1/2)g(\Delta t)^2$  to solve for  $v_1$ , we found a speed  $v_1 = 7.48 \pm 0.37$  m/s at position  $y_1$ , which in this case is 4 cm below the lower end of the nozzle. At this point we made the assumption that the particles start moving freely at about the same height in this pressurized flow case as they did in the unpressurized case. If this is valid, the kinetic energy/mass acquired by the particles due to conversion of gravitational potential energy would be  $gh = 9.80 \text{ m/s}^2 \times (0.21 \text{ m} + 0.04 \text{ m}) = 2.45 \pm 0.17$  J/kg. This corresponds then to a gravitational power input of  $P_{\text{grav}} = \dot{m}_s gh = 0.78 \text{ kg/s} \times 2.45 \text{ J/kg} = 1.91 \pm 0.15$  W, not including uncertainty in  $\dot{m}_s$ .

The total power in the particle flow at the position  $y_1$  is  $P_{\text{total}} = (1/2)\dot{m}_s v_1^2 = 21.8 \pm 2.2$  W, so the power due to energy transfer from the compressed gas would be  $P_{\text{gas}} = P_{\text{total}} - P_{\text{grav}} = 19.9 \pm 2.2$  W. The converted fluid specific energy would then be  $w_e = 25 \pm 3$  kJ/kg, not including uncertainty in the mass flow rate of the gas, and the corresponding efficiency relative to an ideal isothermal process would be  $e_i = 23 \pm 3\%$ .

Note that this is all based on one set of measurements, and so we don't know how reproducible the values actually are. In other words, the uncertainties in the measurements are not all that well determined at this point.

The ability to convert the energy of a compressed gas into other forms has been demonstrated experimentally by connecting the turbine to a dynamometer as illustrated in Fig. 1. The dynamometer used in



**Figure 3.** High-speed photograph of two-phase fluid passing through a turbine under pressure. The readout of a tachometer is visible in the upper left corner.

the experiment is similar to one used previously.<sup>17</sup> A low overall energy conversion efficiency, a few percent at most, is attributed to the type of turbine used. Use of an impulse turbine such as Pelton-type turbine is planned for future work.

### III. Turbine Erosion

A measurement was made of a turbine erosion rate. The turbine used for the measurement is made of 316 stainless steel, and has a diameter and pitch of 7.6 cm. The turbine was first thoroughly cleaned using a fine-hair brush and blasted with compressed air to remove adhered particle contaminants. It was weighed using a Mettler-Toledo XS205 precision balance set to 0.01 mg resolution to establish a baseline mass. The turbine was then immersed in a particle-filled hopper for about five seconds; was then removed, brushed down, blown clean with compressed air, and re-weighed. This process was repeated multiple times to establish the turbine's average mass (with experimental uncertainty),  $108.4978 \pm 0.0011$  g, subject to exposure to the hopper full of particles. As the particles had no velocity, this procedure should not erode the turbine. Experimental uncertainty larger than the resolution of the balance is attributed to adhesion to the turbine's surface of unobserved contaminants resulting from alternating exposure to the particle hopper, the cleaning processes, and the laboratory environment.

The turbine was fixed in place within the experimental apparatus so it could not rotate, and one blade was positioned directly under the nozzle. In normal operation, the turbine would be spinning, and its blades would present a relative velocity to the particles lower in magnitude than when the blades are fixed. Higher relative velocity between the particles and blades corresponds to more prevalent blade erosion. Therefore, by preventing turbine rotation in this test, maximum relative velocity is achieved, and the result is an upper bound on the expected erosion rate for the real functioning system. The particles were loaded into the apparatus' hopper reservoir, which was then pressurized to 377 kPa with compressed air and maintained at that value during the experiment by a pressure regulator. The experiment commenced by opening a valve, which trained a jet of the two-phase fluid on the fixed turbine blade at constant volume flow rate. After striking the fixed turbine blade, the particles were collected in a particle separation chamber and ultimately weighed using an Ohaus Scout Pro balance (with 1 g resolution) to establish the weight of particles used. As the experiment was not rigged for continuous operation, the process was repeated three times, streaming a total of  $22,273 \pm 15$  grams of particles over the fixed turbine blade.

Between each streaming event (each event used approximately 7500 grams of particles), the turbine was recovered from the apparatus and its set screws removed to release particles that may have accumulated in the threads. To eliminate additional adhered particles, the turbine was tapped against a solid surface, cleaned with the fine-hair brush, and blasted with compressed air. It was then weighed on the Mettler-Toledo XS205 precision balance to establish mass lost due to erosion. Reported results are the cumulative outcome from all three identical particle streaming events.

The final turbine mass,  $108.4958 \pm 0.0011$  grams, indicates a total mass reduction from erosion of no more than  $0.0020 \pm 0.0022$  grams. The erosion mass with respect to the streamed particle mass was  $9.0 \times 10^{-5}$  mg/g. As a basis of comparison, this erosion rate is over 6600 times smaller than a rate reported on the same unit basis by Ghenaïet et al. for MIL-E5007E sand particles (0 - 1000  $\mu\text{m}$  diameter) impacting a rotating cast aluminum impeller.<sup>13,14</sup> By way of comparison, we approximate the lifetime of a turbine in our system by extrapolating the efficiency drop Ghenaïet et al. observed over 9 hours at an average erosion rate of 0.843 mg/g. This extrapolation suggests similar degradation might be expected for the turbine of our system after 9.52 years. Moreover, the 7.1% adiabatic efficiency reduction Ghenaïet et al. observed after 9 hours resulted primarily from aerodynamic performance degradation. The aerodynamic characteristics of our subsonic turbine are not critical to its proper operation, and performance degradation of our turbine should therefore be slower than the aerodynamic degradation observed by Ghenaïet et al. Recall also that our measurement yields the maximum erosion rate because the turbine was fixed. For these reasons, the true turbine performance degradation for our system should be much slower than the 0.75%/year reduction (at 100% utilization) suggested by the analysis. We conclude that manageable erosion rates may be possible for the system illustrated in Fig. 1.

## IV. Concluding Remarks

The energy conversion process reported here may be ideally suited, in the long term, for incorporation into a cryogenic heat engine. A cryogenic heat engine can convert heat obtained from the atmosphere into useful work by employing a cryogenic-temperature substance as a heat sink. The concept has been demonstrated with the University of North Texas “CooLN2Car” and the University of Washington “LN2000,” each a zero-emission vehicle that uses liquid nitrogen as a “fuel.” Operation of the cryogenic heat engine in the CooLN2Car is similar to operation of an open (Rankine) cycle steam engine. In an open cycle steam engine, water is vaporized under pressure to produce compressed gas (steam). When operating the CooLN2Car open cycle cryogenic heat engine, atmospheric heat is used to vaporize liquid nitrogen under pressure to produce compressed nitrogen gas. In both cases, the energy of the compressed gas is used to power the vehicle, and the exhaust gas is released into the atmosphere. The CooLN2Car’s primary limitation is its limited driving range, which is 24 km between refills of a 180 L liquid nitrogen tank.

A fuel option for a cryogenic heat engine is liquefied air. Air is composed of 78% nitrogen and 21% oxygen, and liquid nitrogen and liquefied air have similar fuel properties for cryogenic heat engines. It is less expensive to produce liquefied air than liquid nitrogen, because oxygen does not have to be separated during the liquefaction process. Also, the required modifications to a conventional liquid nitrogen tank to allow it to store liquefied air without preferentially venting nitrogen appear to be relatively simple.<sup>17</sup>

Widespread use of liquefied air as a fuel is a rather appealing prospect. It would provide a long-term potential to reduce greenhouse gas emissions or possibly even to *reverse* environmental impacts associated with the increase of greenhouse gases in the atmosphere, provided non-polluting energy sources are used to produce the fuel. Greenhouse gases are necessarily separated during the liquefaction process, providing a possible avenue for carbon dioxide sequestration.

A typical multi-kilowatt low-speed air motor, such as the Gast 16AM-FRV-13 vane-type motor that is currently used in the CooLN2Car, provides a maximum specific work of approximately 40 kJ/kg for nitrogen gas. If an isothermal expansion is possible with the system illustrated in Fig. 1 at 293 K, and the gas changes from an initial pressure of 20 MPa to atmospheric pressure (0.10 MPa), then the ideal specific work done by the gas would be 460 kJ/kg. Consider that a single-stage adiabatic expansion within a conventional turbine would provide an ideal specific work of 237 kJ/kg when expanding nitrogen gas with an initial temperature and pressure of 293 K and 20 MPa. To achieve near-isothermal expansion using conventional turbines, multiple stages and gas reheats would be required. Considering the complexity and cost of using multiple high-speed turbines with aerodynamic blades, a single or multiple low-speed turbines with the system illustrated in Fig. 1 may have considerable advantages. We conclude that a possible long-term application of gas expansion and energy conversion in a multiphase fluid may eventually include the development of vehicles that use liquefied or compressed air for short-range zero-emission operation and combustion-based fuels for long-range operation.

In summary, initial research has been reported on isothermal expansion and energy conversion of a gas-solid flow through a nozzle. During the expansion, the energy of compressed gas is converted into kinetic energy of particles. The particles travel at a subsonic speed, serve as a heat exchange medium, and are recycled. The gas-solid flow is directed at a low-speed turbine, which converts the kinetic energy of the particles into other forms.

## Acknowledgments

The authors would like to thank Ron DiIulio for taking the high-speed photos of the two-phase flow and Andrew Farris for his assistance in imaging and characterizing the particles.

## References

- <sup>1</sup>L.-S. Fan and C. Zhu, “Principles of Gas-Solid Flows,” Cambridge University Press, New York, 1998.
- <sup>2</sup>G. I. Parslow, D. J. Stephenson, J. E. Strutt, and S. Tetlow, “Investigation of Solid Particle Erosion in Components of Complex Geometry,” *Wear* **233-235**, 737-745 (1999).
- <sup>3</sup>G. Grant and W. Tabakoff, “Erosion Prediction in Turbomachinery Resulting from Environmental Solid Particles,” *Journal of Aircraft* **12**, 471-478 (1975).
- <sup>4</sup>L. J. W. Graham, D. R. Lester, and J. Wu, “Quantification of Erosion Distributions in Complex Geometries,” *Wear* **268**, 1066-1071 (2010).

<sup>5</sup>H. Z. Li, J. Wang, and J. M. Fan, "Analysis and Modeling of Particle Velocities in Micro-Abrasive Air Jet," *International Journal of Machine Tools and Manufacture* **49**, 850-858 (2009); and references therein.

<sup>6</sup>L. Wang and D. Y. Li, "Mechanical, Electrochemical and Tribological Properties of Nanocrystalline Surface of Brass Produced by Sandblasting and Annealing," *Surface and Coatings Technology* **167**, 188-196 (2003).

<sup>7</sup>V. S. Hegde and R. A. Khatavkar, "A New Dimension to Conservative Dentistry: Air Abrasion," *Journal of Conservative Dentistry* **13**, 4-8 (2010).

<sup>8</sup>A. Hamed, W. Tabakoff, and R. Wenglarz, "Erosion and Deposition in Turbomachinery," *Journal of Propulsion and Power* **22**, 350-360 (2006).

<sup>9</sup>I. G. Wright, "High Temperature Erosion in Coal Combustion and Conversion Processes: Review," *Materials Science and Engineering* **88**, 261-271 (1987).

<sup>10</sup>I. G. Wright, C. Leyens, and B. A. Pint, "An Analysis of the Potential for Deposition, Erosion or Corrosion in Gas Turbines Fueled by the Products of Biomass Gasification or Combustion," *Proceedings of the ASME Turbo Expo 2000*, Paper No. 2000-GT-0019 (2000).

<sup>11</sup>W. Tabakoff, "Investigation of Coatings at High Temperature for Use in Turbomachinery," *Surface and Coatings Technology* **39-40**, 97-115 (1989).

<sup>12</sup>G. O. Musgrove, M. D. Barringer, K. A. Thole, E. Grover, and J. Barker, "Computational Design of a Louver Particle Separator for Gas Turbine Engines," *Proceedings of ASME Turbo Expo 2009*, Paper No. GT2009-60199 (2009).

<sup>13</sup>A. Ghenaiet, S. C. Tan, and R. L. Elder, "Experimental Investigation of Axial Fan Erosion and Performance Degradation," *Proceedings of the Institution of Mechanical Engineers, Part A: Journal of Power and Energy*, **218**, 437-450 (2004).

<sup>14</sup>A. Ghenaiet, S. C. Tan, and R. L. Elder, "Prediction of an Axial Turbomachine Performance Degradation Due to Sand Ingestion," *Proceedings of the Institution of Mechanical Engineers, Part A: Journal of Power and Energy*, **219**, 273-287 (2005).

<sup>15</sup>Y. Ding, Z. Wang, M. Ghadiri, and D. Wen, "Vertical Upward Flow of Gas-Solid Two-Phase Mixtures Through Monolith Channels," *Powder Technology* **153**, 51-58 (2005).

<sup>16</sup>G. E. Klinzing, F. Rizk, R. Marcus, and L. S. Leung, "Pneumatic Conveying of Solids A Theoretical and Practical Approach," Third Edition, Springer, New York, 2010; and references therein.

<sup>17</sup>M. C. Plummer, C. P. Koehler, D. R. Flanders, R. F. Reidy, and C. A. Ordonez, "Cryogenic Heat Engine Experiment," *Advances in Cryogenic Engineering* **43**, 1245-1252 (1998).

<sup>18</sup>C. A. Ordonez, "Liquid Nitrogen Fueled, Closed Brayton Cycle Cryogenic Heat Engine," *Energy Conversion and Management* **41**, 331-341 (2000).

<sup>19</sup>C. A. Ordonez, M. C. Plummer, and R. F. Reidy, "Cryogenic Heat Engines for Powering Zero Emission Vehicles," *Proceedings of the 2001 ASME International Mechanical Engineering Congress and Exposition*, Paper No. IMECE2001/PID-25620.

<sup>20</sup>M. C. Plummer, C. A. Ordonez, and R. F. Reidy, "Liquid Nitrogen as a Non-Polluting Vehicle Fuel," *Proceedings of the 34th Intersociety Energy Conversion Engineering Conference*, SAE Paper No. 1999-01-2517 (1999).

<sup>21</sup>C. A. Ordonez and M. C. Plummer, "Cold Thermal Storage and Cryogenic Heat Engines for Energy Storage Applications," *Energy Sources* **19**, 389-396 (1997).

<sup>22</sup>C. A. Ordonez, "Cryogenic Heat Engine," *American Journal of Physics* **64**, 479-481 (1996).

<sup>23</sup>C. Knowlen, A. T. Mattick, A. Hertzberg, and A. P. Bruckner, "Ultra-Low Emission Liquid Nitrogen Automobile," SAE Paper No. 1999-01-2932 (1999).

<sup>24</sup>C. Knowlen, A. T. Mattick, A. P. Bruckner, and A. Hertzberg, "High Efficiency Energy Conversion Systems for Liquid Nitrogen Automobiles," SAE Paper No. 981898 (1998).

<sup>25</sup>C. Knowlen, J. Williams, A. T. Mattick, H. Deparis, and A. Hertzberg, "Quasi-Isothermal Expansion Engines for Liquid Nitrogen Automotive Propulsion," SAE Paper No. 972649 (1997).

<sup>26</sup>J. Williams, C. Knowlen, A. T. Mattick, and A. Hertzberg, "Frost-Free Cryogenic Heat Exchangers for Automotive Propulsion," AIAA Paper No. 973168 (1997); and references therein.

<sup>27</sup>M. D. Abramoff, P. J. Magalhaes, and S. J. Ram, "Image Processing with ImageJ," *Biophotonics International* **11**, 36-42 (2004). [see also <http://rsb.info.nih.gov/ij/>].